Internal Report
DESY F41
HASYLAB 80/04
May 1980

Soft X-Ray Contact Microradiography

Eigentum der
Property of DESY Bib...
Zugang:
Accessions: 30. JUNI 1980
Leihfrist:
Loan period: 7 Tage
days

by

W. Gudat

DESY behält sich alle Rechte für den Fall der Schutzrechtserteilung und für die wirtschaftliche Verwertung der in diesem Bericht enthaltenen Informationen vor.

DESY reserves all rights for commercial use of information included in this report, especially in case of apply for or grant of patents.

"DIE VERANTWORTUNG FÜR DEN INHALT
DIESES INTERNEN BERICHTES LIEGT
AUSSCHLIESSLICH BEIM VERFASSER."

Soft X-Ray Contact Microradiography

W.Gudat

Institut für Festkörperforschung der

Kernforschungsanlage Jülich GmbH,

D-5170 Jülich 1

West Germany

to be published in

Uses of Synchrotron Radiation in Biology

edited by H.Stuhrmann

Academic Press, Inc. (London)

Soft X-Ray Contact Microradiography

Contents:

1. Introduction

2. The Technique

3. Photon Interactions

   contrast mechanism

   radiation damage versus resolution

4. Resists

   sensitivity and contrast

   resolution

5. Resolution of the Technique

6. Applications

7. Summary and Outlook

References

Tables

Figure Captions

Figures

1. Introduction

The availability of high resolution electron microscopes in the early fifties opened up a new dimension of ultrastructural research in modern biology. Although extremely important results have been obtained, the remarkable progress in microbiological and biophysical research has slowed down somewhat or perhaps has become limited. This appears to be due to the fundamental physical problems which are encountered when biological cells or macromolecular structures are to be investigated with electron microscopes. Structural information is mainly obtained from elastic electron scattering events, while inelastic scattering provides compositional information. The small average atomic number of biological material strongly favours the occurance of inelastic scattering events. Since these inelastic processes also cause severe molecular damage of biological material, electron beam damage appears to be the fundamental problem in high resolution electron microscopy /1,2/. In general, the same statement also holds for X-ray microscopy. However, as investigations indicate / 3 / the radiation damage with X-rays is much smaller in a suboptical regime than with electrons at a comparable resolution. This is one of the important reasons for the increasing efforts in these days for ultrastructural research with X-ray microscopy.

In particular for soft X-rays in the range 1-10 nm there are some other favorable reasons for microscopy of biological material. These include: A spatial resolution as good as about

10nm; large penetration depth of X-rays which allows the visualization of the interior structure of whole organelles or cells; a wavelength dependent contrast high enough to study even unstained specimens.

The possibilities of soft X-ray microscopy have already been realized very early and they were the driving force for the development of various techniques. The simplest and oldest one is called contact microscopy and dates back to the turn of century /4/. Goby /5/ used X-rays to expose a photographic emulsion with a specimen placed on top of it. After development he viewed the film in an optical microscope. Since these early attemps various methods have been explored and applied to obtain magnified images with use of X-rays including projection techniques, grazing incidence mirror optics and scanning systems. The obtained resolution was comparable to that of a light microscope. The field of microscopy with X-rays from conventional sources has been carefully reviewed / 6-8/. More recently specifically biological and medical aspects have been discussed / 9-11 /.

In 1972 Horowitz and Howell /12/ demonstrated that synchrotron radiation can advantageously be used for soft X-ray microscopy. Since that time a remarkable renewal of interest in X-ray microscopy has occured accompanied by considerable progress. In 1976 the feasibility of contact microscopy at 10 nm resolution has been demonstrated /13/ by using plastique photosensitive

resist materials and scanning electron microscopes. Zone plates as optical elements can already produce magnified soft ray images directly at a resolution of 70nm /14/. Microscopy techniques utilizing zone plates, grazing incidence mirrors, normal incidence mirrors with multilayer coating /15/ and holography /16/ are thought to allow an optimum resolution of the order of 10 nm. An up to date discussion of the latter methods is presented in the chapter by Schmahl et al /17/. and by Kirz and Sayre /18/. Brief reviews are available in the literature /19-21/. In this chapter we want to give an overview only on the method of soft X-ray contact microscopy.

This chapter is organized as follows: In Sect. 2 the general technique is described. The important topics of photon interactions resulting in contrast formation and radiation damage are treated in Sect. 3. We describe the properties of X-ray resists in Sect. 4 and consider the attainable resolution of the technique in Sect. 5. Then we proceed to discuss selected experimental results along with some important technical details. Finally we compare contact microscopy to other techniques and give some future developments.

2. The Technique

Contact microradiography (CM) in its present form is a natural extension of the early work described in refs./5-11/. Shortcomings in the early studies were due to poor resolution and sensitivity of X-ray detectors, insufficient intensity and collimation of X-ray sources especially in the relevant soft X-ray region from .1 to 10 nm and due to the use of optical microscopes for inspection of the micrographs. These shortcomings have now largely been elliminated /22/. Synchrotron radiation, already available from dedicated storage rings, provides a high flux of soft X-ray radiation which is well collimated and of very high brightness. We will not go here in any detail, since a full discussion of the properties of synchrotron radiation is presented by Materlik in chapter 1 /23/. X-ray sensitive organic polymers with high resolution capabilities have been developed in connection with electron beam- and X-ray lithography which are present day technologies to produce microstructures for electronic circuits /24/.

The experimental arrangement for CM is shown schematically in Fig. 1. In contrast to most of the other microscopy techniques, mentioned above, for CM in its simplest form optical components are not required between source and specimen and detector. An extremely smooth material (mostly silicon or glass) serves as substrate for a thin film of organic polymer . This film, called resist[+] acts as a high resolution, position and X-ray sensitive

[+] In X-ray and e-beam lithography the resist has to protect the underlying Si material in subsequent processing steps, i.e. the material is resistent to acids, etc.

detector. Specimens placed on top of the resist are exposed to a beam of collimated soft X-rays (Part I, Fig. 1) at about normal incidence. The transmitted spectral intensity depends on the absorption properties of the specimen. A small fraction of this intensity is absorbed in the resist and modifies the molecular structure of the material in such a way that it becomes more soluble in exposed regions than in unexposed. After removel of the specimen, a 3dimensional replica of the specimen's optical density is thus obtained at unit magnification via the development procedure (Part II, Fig. 1). The inspection of the replica and thus the magnification is most easily obtained with a scanning electron microscope (SEM) thereby taking advantage of the large depth of focus of the SEM. Since polymers are non-conductors the resist pattern has to be metallized prior to the SEM work in order to avoid charging in the electron beam.

Various kinds of specimen have been investigated, since the first demonstration of the technique /25/ using either synchrotron radiation /13,21,22,26-32/ or X-rays from conventional sources /13,20,26,29,31-33/. Some of the results will be discussed in the following sections. Here we show in Fig.2 as an example the replica of a diatom /26/ obtained with synchrotron radiation from the DESY synchrotron with an exposure time of about 10 min. In contrast, exposure times for similar specimen with carbon K_α radiation are in the order of 20 hours. Structural details smaller than 100 nm can already be seen on the resist replica. It is important to note, that the height of the resist replica, as seen with the SEM, is not only related

to the thickness of the specimen but also to the X- ray absorption coefficient. We will discuss this in more detail lateron.

X-ray microscopy set-ups with conventional sources have been described /7-11/. A schematic of an experimental station for CM at a synchrotron radiation beam line is shown in Fig. 3. The exposures are performed in evacuated sample chambers, which are connected with long beamlines to the accelerator. At typical distances of 10 to 40 m, there are several square centimeters for X-ray exposures available. If the specimen is placed in direct line of sight to the radiation source point, it is exposed to the full spectrum of synchrotron radiation. As described in chapter 1, this covers the range from the visible to wavelengths of about 0.1 nm at an electron energy in the accelerator of about 1 GeV. It is adventageous to use a smaller spectrum for the resist exposure. One would like to utilize a soft X-ray monochromator with a broad bandpath. Since such instruments are not yet readily available, grazing incidence mirrors have been applied as short wavelength cutoff elements or a combination of conventional absorption edge filters. At DESY a beamline with a 4° grazing incidence mirror is available which delivers soft X-rays down to about 2 nm /22/. In that beamline the exposure for the replica in Fig. 2 has been carried out.

3. Photon interactions

Contrast mechanism

The attenuation of soft X-rays in the wavelength range 0.5 to 10 nm is almost completely due to photoabsorption. Scattering events are by 4-5 orders of magnitude more seldom. Thus X-rays penetrate material on straight lines. This is important for X-ray transmission microscopies like CM.

The absorption of X-rays is described by Lambert-Beer's law

$$I = I_o \exp(-\alpha d) = I_o \exp(-\alpha/\rho \cdot m)$$

I_o is the intensity of the unattenuated beam and I is the intensity transmitted through matter of density ρ, thickness d, linear absorption coefficient α and mass absorption coefficient (α/ρ). The mass per unit area of the absorber is $m = \rho \cdot d$. The absorption coefficients are strongly wavelength and atomic number Z dependent quantities. Fig. 4 gives a collection of such data for several materials /34,35/. For low Z materials the well-known saw tooth behaviour is observed in this wavelength range. This is a justification to calculate the total mass absorption coefficient for materials of different elements by a weighted superposition; i.e. $(\alpha/\rho)_t = \sum_i a_i (\alpha/\rho)_i$ with a_i the weight fractions. At the long-wavelength side one observes for high Z materials deviations from the saw tooth behaviour /34/. The invers of α is the penetration length of the radiation. From Fig. 4 it is seen

that biological tissues of a few μm thickness still transmitt a considerable fraction of incident soft X-rays, in contrast to high Z materials. Thus the spectral dependence of the absorption of composite elements of a specimen provides a differential contrast. Obviously, the choice of a particular wavelength range is important for CM. The investigation of biological material in its natural state; i.e. wet, is favourably done in the range from 2,3 to 4,3 nm, where water absorbs much less than protein. The preferred wavelength range for high resolution transmission microscopy with high contrast is clearly the soft X-ray range $\lambda \gtrsim 1$ nm. This has already been pointed out by several workers in the past /9-11,36-38/.

Similar considerations provide the basis for microchemical analysis of specimen. Quantitative work in this field is most easily accomplished with tunable soft rays of sufficient bandwidth which is available from synchrotron radiation sources. An exposure below and above an absorption edge provides a calibration of the measured intensity and the weight fraction of the material can readily be evaluated. Careful reviews of microchemical analysis work up to 1970, carried out with conventional X-ray sources, have been provided /8-11/.

Radiation damage versus resolution

The absorption of energetic photons in the range 1-10 nm gives rise to the creation of "holes" in closely bound core electron shells and/or to energetic electrons from valence shells. Holes are filled in subsequent fluorescence- or Auger processes, which again create fast electrons. If the latter are energetic enough they might produce further electrons in collisions with electrons from neighbouring atoms. Finally excited atoms can be left behind in a "cloud" of scattered electrons. All the processes have a certain probability to irreversably change the chemical bonding of the molecular structure, which can give rise to emission of ions,to free radicals etc. Thus always a certain radiation damage occurs. This is precisely what happens in the photo resist material while being exposed to soft X-rays. In that case radiation damage is used to form an image of a specimen in a development procedure.

As already pointed out in the introduction, radiation damage is the most severe problem in sub-microstructural research of biological material. In spite of this only very little is known, in particular experimentally. The available information will be discussed by Halpern in chapter 11 /39/. But due to the importance we want to summarize some of the considerations given by Sayre et al. /3,40/.

Specimen of low differential contrast require a large photon flux in order to distinguish small features in the image. For microscopy of biological objects it is therefore important to select a proper spectral range, which minimizes the radiation damage to the specimen and optimizes the signal to noise ratio in the image at a given resolution. Sayre et al / 3 ,40/ did a quantitative model calculation on a water-protein object in order to study this problem. We reproduce some of their remarkable results in Fig. 5. The feature under investigation is a protein cube in a water background. For simplicity of the calculation the feature thickness t_F has been assumed to be equal to the resolution d. The thickness versus resolution (t,d) diagram of Fig. 5a shows the incident photon flux required to give a visibility of the feature with a signal to noise ratio $S/N \gtrsim 5$. As expected, with increasing flux higher resolution becomes available from 2.7 to 4.2 nm. In the same wavelength range a flux of 10^3 photons/nm^2 is necessary for a resolution of $\sim$10 nm, almost independent of specimen thickness (for $t \lesssim 10$ nm). For comparison, at the DESY synchrotron where contact microradiography at 10 nm resolution has been demonstrated /13/ (compare Fig.12 ,exposure time 15 min) a spectral integrated flux (2.7 to 4.2 nm) of about 1 phot/sec nm^2 is available in a distance of 40 m in a field of about 5x2 cm^2. Fig. 5b shows the conversion of the photon flux in the (t,d) curves of Fig. 5a to absorbed energy in a volume element per mass unit. More familiar this is called the absorbed dose (1 rad = 10^{-5} J/g) (see also Sect. 4).

To get an idea of the feasibility of high resolution microscopy on live biological specimen, we should compare the required dose of 10^4 J/g for a 10 nm resolution with the "survival-dose". The most radiation resistant living cells are killed by a dose of about 10 J/g for irradiation with electrons /1,39/. Assuming the same killing rate for soft X-ray exposure, 10 nm resolution appears not to be feasable even at a reduced signal to noise ratio. In this context we have to note that in the calculation of Sayre et al. a detector efficiency $\mathcal{E}$ = 1 /41/ has been assumed which definitely cannot be obtained in CM /42/. It is important however, to realize that wet specimens likely can be imaged at 10 nm resolution with transmission microscopy techniques with tolerable radiation damage. In contrast, in transmission electron microscopy the obtainable resolution is limited to 100 nm at the same dose $\sim 10^4$ J/g for comparable specimen thickness and radiation damage /40/.

4. Resists

In the history of CM various efforts have been made to improve on the speed and resolution of the X-ray detectors /43-45/. Notably the work of Ladd et al /43/ is mentioned where X-ray images had been obtained at submicrometer resolution and viewed with transmission electron microscopes. The break through in high resolution X-ray sensitive detectors is closely linked to industrial needs for replication of micron structures on masks for electronic circuit production. In systematic research various materials called resists have been found with either high sensitivity or high resolution or both at more moderate level /24/ (see also Table 1).

All resist materials in practical use are thin films of organic polymers /46/. Polymethylmethacrylat (PMMA) /47/ is an extensively used resist in both, the technical application like electron beam and X-ray lithography, and in microscopic application like contact microradiography. This again shows that both techniques are closely related. Only few other organic photo resists have been used for CM /e.g. 22, 30,48/.

PMMA is a polymerization product with a summation formula $-(C_5H_8O_2)_n-$. (For microscopy applications one uses Dupont Elvacite 2041 with n about 10 000.) Resists are easily prepared in various thicknesses by spin coating onto smooth substrates (highly polished silicon or glass) with a solution of PMMA in chlorobenzene, followed by drying at about 160°C. Resist thickness for microscopical application is typically 20 nm to 100 nm, while for X-ray lithography several 100 nm is preferred because of subsequent processing steps.

As described in the previous section, the absorption of soft X-rays results in a shower of fast secondary electrons, with still enough energy to damage molecules. This is the reason that resists developed for electron exposure, are also good X-ray resists. Without going into details which can be found in ref. /24,46,47/, one can say that the soft-X-ray exposure results in chain scission of the PMMA molecules, thereby lowering the molecular weight. This in turn leads to a higher solubility of the PMMA in the developer liquid (here methylisobutylketone (MIBK) diluted in isopropanole (IPA)).

Thus exposed areas of the resist will dissolve more rapidly, than unexposed parts. This is called a "positive" resist. In "negative" resists cross-linking of molecules occurs upon exposure and exposed areas will become less soluble than unexposed.

Sensitivity and Contrast

There are three important quantities which characterize a photoresist: the sensitivity, the contrast and the resolution. The former two can be defined by means of the dissolution rate S of the resist as a function of the exposure. Fig. 6 shows this curve for PMMA. Here the upper scale gives the exposure F (in J/cm^2) at the top of the resist, while the lower scale gives the exposure W in a volume element, i.e. the absorbed power. Both scales are linked by the relation $W = F \cdot \alpha$, with α being the linear absorption coefficient (see Fig.4). In concentrated MIBK developer unexposed PMMA dissolves at a rate $S_o \simeq (7 \pm 2.5)$ nm/min. Exposure increases the dissolution rate first slowly, but then stronger and stronger and a weaker developer has to be used. A rate of about 1000nm/min is obtained at an exposure of 5000 J/cm in a (3:1) developer solution /22/. A peculiarity of PMMA is also evident from Fig. 6 . At exposures above 5×10^4 J/cm^3 the resist starts to become less soluble than at lower exposures. At 10^5 J/cm^3 it behaves like a negative resist, while normally it is positive. Now the sensitivity is related to the ratio $S(F_2)/S(F_1)$ of dissolution rates at adjacent areas of the resist with exposure F_1 and F_2. In X-ray lithography the mask to be replicated can be produced with a high optical contrast, i.e. adjacent parts are either "clear" or "opaque". Thus to a good approximation $F_1 \approx 0$ and the required exposure giving $S(F_1)/S(0)=10$ is defined as sensitivity. According to Fig.6 for PMMA this is 300 J/cm^3.

The high ratio of dissolution rates due to high contrast of masks results in "vertical walls" in the resist replica as demonstrated in Fig.7. The aspect ratio, i.e. the ratio of height and width of the structures in Fig.7, is an important quantity in the technological application.

Specimen used in CM will in general not provide such a high contrast that $S(F_1) \cong S_o$. In fact, it is the purpose of soft X-ray microscopy to reveal even very small differences in optical contrast. In this case the slope of the dissolution rate versus exposure curve (see Fig.6) becomes the important quantity. The contrast γ of the resist, defined by the relation

$$\lg(S(F_1)/S(F_2)) = \gamma \cdot \lg(F_1/F_2)$$

then determines the ability of the resist to convert a small ratio in exposure $F_1/F_2 \sim T_1/T_2$ to a sizable ratio of heights in the replica. For CM the contrast γ should be as high as possible since the transmittances T_i of adjacent resolution elements of the specimen are both close to 1 due to $T_i = 1 - \alpha_i d_i$ (compare Fig.4). It is important to note that both is required, optical contrast of the specimen and high contrast of the resist. Fig.6 demonstrates that the contrast γ is a function of exposure and developer concentration. The optimum exposure does not only depend on the dissolution characteristic, but also on the desired resolution and radiation resistivity of the sample, since for a statistically significant image the dose absorbed by the specimen must equal or exceed the resist dose. With this in mind, an absorbed dose slightly above 1000 J/cm^3 appears to be appropriate.

Fig.8 gives an example of the influence of soft X-ray exposure on the dissolution of PMMA in the case of a specimen with weak contrast. Micrographs of latex spheres of 500 nm diameter mounted on 300 nm collodion film supported by a 34 μm Cu mesh, have been obtained with monochromatized synchrotron radiation of wavelength $\lambda = (4.6 \pm 0.1)$ nm in a focussed beam /49/. Part a of Fig.8 shows a well exposed region of the replica, while part b shows a heavily over-exposed region of the same replica. The 1 μm thick resist is dissolved down to the substrate in exposed parts. The image of the optical density of the latex spheres has turned into the column-like structures about 300-400 nm wide and up to 850 nm high. The steep edge showing the full height of the resist is caused by the Cu mesh. The grainy structure of average size $\sim$75 nm has been found as due to the collodion support film. Fig.8 demonstrates that close control of the exposure and the development procedure is necessary, in particular for quantitative work. It further shows that the dissolution is a 3 dimensional property and that side way attack of the resist occurs also /24,29/.

The dissolution rate curves of Fig.7 have been obtained with the assumption that all soft X-ray wavelengths have the same effect provided the exposure (in J/cm^3) is the same /22,24/. Fig.9 shows the dissolution rate of PMMA as a function of exposure time in different spectral ranges which were obtained by means of transmission filters in connection with grazing incidence reflection /49/. The data show that the contrast increases to a maximum value $\gamma \sim 3.6$ with decreasing spectral range centered around the carbon K-edge. To further study the spectral

dependence of the contrast, one can evaluate the latex replica displayed in Fig. 8b by making use of the relation /24/

$$d_{norm} = \frac{d_{remain}}{d_o} = 1 - T_{sp}^{\gamma}$$

for the so called normalized remaining resist thickness d_{norm} for a low contrast specimen (transmission $T_{sp} \rightarrow 1$). This indicates that for PMMA $\gamma \simeq 7$ for $\lambda = (4.6 \pm 0.1)$ nm.

Due to the particular importance of the resist contrast for CM the question on the wavelength dependence of γ warrents further detailed studies.

Resolution

The third important quantity needs to be discussed, namely the resolution of the resist. Spiller and Feder /24/ present a discussion for the performance of an ideal resist and they relate the required average number of photons $\bar{n}$ absorbed in one resolution element Δ^3 of resist to the exposure density F by

$$\bar{n} = \frac{F \cdot \alpha \cdot \Delta^3}{\hbar\omega} = \frac{W \cdot \Delta^3}{\hbar\omega} .$$

With a value $W \sim 500$ J/cm^3 at $\lambda \sim 4.4$ nm they obtain ~ 1.4 absorbed photons per 5 nm resolution element.
At sufficiently high exposures the resolution is practically limited by the effective range of the photo excited electrons (compare Sect.3), since the resist is "exposed" by secondary electrons. The range of hot electrons is strongly energy dependent /50/ while the maximal energy is closely related to the photon energy. Therefore the resolution of the resist is also wavelength dependent. This has to be considered when the spectral range of optimum resolution is to be used /21/.

Experimental results for PMMA /51/ show that the range of hot electrons is smallest at λ= 4.5 nm with a value of 5 nm. At λ = 0.83 nm and 0.46 nm it becomes already 35 nm and 65 nm, respectively. Since the range of electrons when excited by soft X-rays, does not change very much with composition of the material /52/ the value of 5 nm can be considered as the best obtainable resolution in CM.

In Table 1 we finally summarize various properties of PMMA and compare with several other resists. As already pointed out, only very few of these materials have been used for CM. In particular at a moderate resolution, several resists appear to be useful for CM, since they offer a much higher sensitivity and thus less exposure and radiation damage to the specimen.

5. Resolution of the Technique

The attainable resolution of the technique CM is limited by various factors. In Sect.2 we already discussed that wet biological specimen can at best be examined with a 10 nm resolution due to radiation damage.

However, for dried and eventually stained specimen a better resolution is possible as regards to contrast and shot noise considerations. There are two possible geometrical effects giving rise to a distortion of the shadowgraph of an object /7-11/. The first is penumbral blurring (δ p) due to the finite size of the X-ray source (s). This effect is negligible small ($\delta p < 10$ Å) if collimated synchrotron radiation is used, as seen from the relation $\delta p = s \cdot t/D$, where t is the distance

object-resist and D is the distance source-object. The second effect is due to non-normal incidence of the X-rays onto the sample. It is considered in lithography applications /22/. But again it can easily be made sufficiently small.

More important than the geometrical effects are the behaviour of the resist material and other wavelength dependent effects. The two effects which in all practical cases determine the attainable resolution, are diffraction of the soft X-rays and as pointed out previously (Sect.4), the range of the hot photoelectrons that are promoted in elementary absorption events.

Fig.10 demonstrates the occurance of diffraction effects in the micrograph of latex spheres on collodion coated copper grids obtained with PMMA at a wavelength of 4.6 nm in a focussed beam. Fig.10a shows the edge of the Cu grid on the right and two parallel structures with a distance of about 300 nm. In Fig.10b we observe the same feature in the X-ray image of latex spheres in the form of surrounding ditches. Diffraction effects are clearly visible due to finite distance (several μm) between specimen and resist and due to the monochromatic light.

With intimate contact between sample and resist, the desired geometry for CM, diffraction takes place only in the thickness of the sample itself and the thickness of the photoresist film. In order to investigate the resolution limitation of this case one would have to solve a complicated

diffraction problem. For simplicity we consider the case of an opaque edge intersecting a collimated soft X-ray beam at normal incidence, which at best holds for the edge of the specimen. Fresnel diffraction theory /53/ gives for the distance of the first local intensity maximum $x_m = (t \cdot \lambda)^{1/2}$, with t being the distance between object and resist. Fig. 11 displays the intensity distribution of a Fresnel diffraction case and in addition a curve, normalized to the same maximal height, which accounts for the contrast of the resist. This curve explains the observations of Fig.10. The conclusion then is, considering all the above resolution limiting effects, that the wavelength range for best resolution of 5 nm is at about 2 to 4 nm.

A resolution close to the diffraction limit has already been obtained /13/. Fig. 12 shows a replica obtained from a thin plastic embedded section of frog retinal pigment epithelium upon exposure with wide band pass synchrotron radiation. A moderate resolution SEM has been used to obtain the structures of Fig.12a.In contrast a high resolution low-loss SEM /54/ micrograph (Fig.12b) taken from the same resist replica, shows details in the order of 10 nm even on a single melanin granule, that were completely obliterated in Fig. 12a. Obviously, a resolution of about 10 nm has been obtained.

Fig.12 emphasizes the importance of a high resolution SEM for the resist inspection. Other wavelength independent effects should be mentioned at this point, namely the grain size of the metallization /55/,possibly grain size of supporting thin films, (compare for instance Fig.9) and finally pin-holes and such like in the resist. However, all of latter effects can

be made sufficiently small compared to diffraction effects and the range of hot electrons in resist.

6. Applications

In this section we want to discuss some results obtained with CM and X-ray resists on biological specimen.

First experimental work on CM with X-ray resist has concentrated on demonstrating the potential of the technique, without going into detailed explanation of what is seen on the replica. In more recent efforts the attention was directed towards an understanding of the details of the resist replica as seen with the SEM. It seems clear from the available results that much more experience is needed to properly interprete all the detailed structures which often have not been seen before by any other ultrastructural technique . A quite similar situation has occured in early high resolution application of electron beam microscopy. Since it is important for an understanding of the SEM pictures and the possibilities of the technique, in general, we will also mention some details on the preparation of the specimen.

Panessa and Warren / 56/ addressed themselves to the question on the optimum specimen preparation in order to faithfully reproduce ultrastructural details. They applied various histochemical preparative methods with and without heavy metal staining before embedding the specimen in plastique. Very thin diamond cut sections were put either directly on PMMA resist or by means of a fine support grid. Their results, basically on directly mounted specimen, show that ultrasoft

CM provides an accurate way to image unstained biological specimen at very high resolution ($\sim$10 nm) and to image histochemical reaction products and surrounding tissue at the ultrastructural level. Moreover it was found that even unstained macromolecules, namely unstained, isolated proteoglycan aggregates, could be investigated by means of CM /56/.

Zadunaisky /57/ continued on the investigation of the pigmented granules of the retinal pigmented epithelium (compare Fig. 12 a,b). He concludes that high concentrations of Ca are accumulated in the melanin granules and that the periodicity of the internal structure of the melanin granule as seen by CM reflects the regular structure inside the granule. The latter suggests that Ca could be bound to melanin.

Chemical analysis of iron and titanium by selective X-ray absorption with monochromatized synchrotron radiation has been demonstrated by Polak et al /28,58/ with mineralogical samples at a few micrometer resolution with use of silver based detector material. High resolution microchemical analysis of biological specimen by means of CM has been shown by McGowan et al /29/. Cells from chick embryo hearts dried by the CO_2 critical point method have been replicated with soft X-rays of a carbon K_α source and with broad band synchrotron radiation (1.5 nm $\lesssim \lambda \lesssim$ 4.5 nm). The two replica in PMMA resist which are reproduced in Fig. 13 reveal marked

differences. These are explained in terms of element distribution within the heart of chick embryo cells being picked up due to the wavelength dependence of the absorption cross sections. The pronounced relief contours of the nucleus (N) and the nucleolus (NO) in the cell replica obtained with CK_α radiation reflects strong build up of nucleic acid containing abundantly oxygen and phosphorus atoms. In contrast, the grape like structure to the left of the nucleus in the synchrotron radiation replica is likely to be a group of mitochondria (M) which contain Mg /29/. No doubt that this type of specimen demands a full investigation with tunable synchrotron radiation.

After first CM studies of chromosomes of the Drosophila salivary gland by Feder et al /13/ further investigations on chromosomes have been presented /33,59/. Sedat et al /59/ studied interphase chromosome structure in polytene and diploid nuclei with the result that polytene chromosomes are ordered structures with a likely fiber subunit- architecture. Manuelidis et al /33/ investigated soft X-ray (carbon K_α) images of purified interphase human nuclei and chromatin on PMMA resist. They compared the results obtained by SEM examination of the resist image with those utilizing more conventional methods, e.g. transmission-, scanning- and high voltage electron microscopy and various light microscopic techniques. Naked nuclei and chromosomes were obtained from different human neuroectodermal tumor tissue culture lines in a sequence of preparation steps. Samples for CM were prepared by putting nuclei concentration

either directly onto PMMA resist or onto electron microscope grids coated with formvar or collodion. While direct mounting in principle allows for best CM results, it gives rise to problems in the removal of the specimen prior to resist development /29,33,49/. On the other hand, grid mounting can result in loss of resolution and can add unacceptable absorption backgrounds (compare Sect. 4). The resist images revealed orderly arrays of absorption profiles in the 3 dim. specimen. Dense chromatin at the edge of interphase nuclei showed aligned periodic peaks of about 220 nm diamter with substructure of the order of 60 nm, as seen in Fig. 14. Dispersed interphase chromosomes also showed absorption periodicities in individual chromosome fibers. In summary, the experiments by Manuelidis et al /33,59/ demonstrated that CM provides new, and additional information into the ordered structure of defined biological specimens.

The ultimate goal of CM is, of course, the investigation of live bioloical specimen. While first successful examinations have already been reported with conventional electron microscopy techniques /60/, there is only mention of a first unsuccessful attempt by the technique of CM /29/. Live chick heart embryo cells have been prepared in a special environmental chamber, similar to previously described systems /61/,and exposed to synchrotron radiation. The resulting replica showed blurred structures and it is believed that this is due to movement of the cells during the 15 minute exposure /29/.

7. Summary and Outlook

The instrumentation seems now to be available to study biological material in a suboptical regime by means of contact microradiography with X-ray resist and scanning electron microscope inspection. In favourable cases, namely at the bottom of the specimen facing the resist, structural details with dimensions as small as 10 nm can definitly be imaged and even 5 nm is possible. However, as present experimental results indicate, much control work must still be done, before proper interpretation of all structural details of the resist image can faithfully be made. Such work includes for instance calibration of geometrical (morphological) shapes, of stain concentrations etc, but also more studies on resist exposure and development characteristics and on the effects of specimen mounting. But this kind of work seems straight forward to be done. Therefore contact-microradiography appears as a very useful supplementing ultrastructural technique. Advantages of the technique certainly include: potentially highest resolution of all practically available soft X-ray microscopy techniques, a complete picture in a single exposure in a very large field, applicability of a wide spectral range from ultra-soft to hard X-rays, the use of "thick" samples for moderate resolution and last not least, a fairly simple experimental procedure.

At this point we should also consider disadvantages of contact microradiography in particular with respect to other available techniques. Obviously, it is not a real-time technique. In fact, the time delay between exposure and development and final resist examination can be made very long. The X-ray resist has a poor detector quantum efficiency which necessarily enhances the radiation dose absorbed by the specimen. In this respect scanning microscopy set ups with high efficiency detectors (e.g. fluorescence detectors, see e.g. /12,17/) are superieur techniques. The attainable resolution is diffraction limited. This implies that in the most interesting spectral range at about 3 nm the resolution of structural details within thick specimen, e.g. wet cells, changes noticeably with distance of the feature to the resist. Finally, the necessity of intimate contact between specimen and resist for best resoltuion renders difficulties in mounting of samples.

Various excellent possibilities of contact microscopy have not been exploited to date, partly due to lake of experimental facilities. With the availability of synchrotron radiation from dedicated storage rings the situation has now changed. First feasibility studies with monochromatized synchrotron radiation have been described in sections 4 and 5. Suitable wavelength scanning systems for a microchemical analysis have been suggested /62,63/. Their realization is presently under investigation. A considerable problem in the interpretation of resist images, namely the fact that the

optical density of the specimen is measured rather than the three dimensional structure, can be tackled by taking stereopairs of images; this means to take several exposures with the specimen tilted with respect to the resist surface /63/. Initial experimental steps have already been done /59/. With further improvements on environmental chambers and with drastically reduced exposure times (<1 sec is possible), the examination of wet cells becomes possible. The laser beam and electric discharge generated plasma X-ray source /64,65/ as laboratory light source is worth mentioning here, since it appears to offer enough flux to expose X-ray resist in a time of less than a msec. The above aspects can very likely be realized with present day technology. A very recent suggestion /66/ to use the resist replica as a special kind of hologram and derive from this by means of SEM magnification and laser reproduction a true three dimensional image, appears to present much more difficulties.

In conclusion, contact microradiography has already proven to have particular merits in ultrastructural investigations and it appears that these merits can be fully exploited in the near future.

Acknowledgement

The author wants to thank Miss A.Franzen for her careful typing of the manuscript and R.Fisseler for help in preparing the figures.

References

/1/ M.S.Isaacson, Specimen Damage in the Electron Microscope, in: Principles and Techniques of Electron Microscopy: Biological Applications, Vol. 7, ed. M.A.Hayat, VanNostrand Reinhold, New York (1977)

/2/ R.M.Glaeser, in: Physical Aspects of Electron Microscopy and Microbeam Analysis, eds.: B.Siegel and D.R.Beaman, John Wiley and Sons (1975)

/3/ D.Sayre, J.Kirz, R.Feder, D.M.Kim and E.Spiller, Science, 196, 1339 (1977),
D.Sayre, J.Kirz, R.Feder, D.M.Kim and E.Spiller, Ultramicroscopy, 2, 337 (1977)

/4/ F.Ranwez, C.R.Acad.Sci. Paris, 122, 841 (1896)

/5/ P.Goby, C.R.Acad.Sci. Paris, 156, 686 (1913)

/6/ P.Kirkpatrick and H.H.Pattey,Jr., in: Handbuch der Physik, ed. S.Flügge, Vol. 30, p.305, Springer Berlin (1957)

/7/ V.E.Cosslett and W.C.Nixon, X-ray Microscopy, Cambridge University Press, Cambridge (1960)

/8/ V.E.Cosslett, X-ray Microscopy, Rep.Progr.Phys. 28, 381 (1965)

/9/ A.Engström, X-ray Microanalysis in Biology and Medicine, Elsevier Publishing, Amsterdam (1962)

/10/ A.Engström, in: Physical Techniques in Biological Research, ed. A.W.Pollister, Vol. III, Part A, p.87, Academic Press, New York (1966)

/11/ T.A.Hall, H.O.E.Röckert and R.L.deC.Saunders, X-ray Microscopy in Clinical and Experimental Medicine, C.T.Thomas, Springfield Ill (1972)

/12/ P.Horowitz and J.A.Howell, Science 178, 608 (1972)

/13/ R.Feder, E.Spiller, J.Topalian, A.N.Broers, W.Gudat, B.J. Panessa, Z.A.Zadunaisky and J.Sedat, Science 197, 259 (1977)

/14/ G.Schmahl, D.Rudolph, B.Niemann and C.Christ, Ann.N.Y.Acad. Sci., to be published

/15/ R.P.Haelbich, A.Segmüller and E.Spiller, Appl.Phys.Lett. 34, 184 (1979)
E.Spiller, Appl. Optics 15, 2333 (1976)

/16/ S.Aoki, Y.Ichihara and S.Kikuta, Jap.J.Appl.Phys. 11, 1857 (1972),
S.Aoki, S.Kikuta, J.J.Appl.Phys. 13, 1385 (1974)

/17/ G.Schmahl, D.Rudolph and B.Niemann, in: Uses of Synchrotron Radiation in Biology, ed. H.Stuhrmann, Academic Press, 1980

/18/ J.Kirz and D.Sayre, Soft X-Ray Microscopy of Biological Specimens, in: Applications of Synchrotron Radiation, eds. S.Doniach and H.Winick, in press

/19/ P.Horowitz, in: Principles and Techniques of Scanning Electron Microscopy, ed. M.A.Hayat, Vol. 5, p.181, Van Nostrand Reinhold, New York (1976)

/20/ E.Spiller, R.Feder and J.Topalian, J.de Physique 39, C4 205 (1978)

/21/ W.Gudat, Nucl. Instrum. and Methods, 152, 279 (1978)

/22/ E.Spiller, D.E.Eastman, R.Feder, W.D.Grobman, W.Gudat and J.Topalian, J.Appl.Phys. 47, 5450 (1976)

/23/ G.Materlik, in: Uses of Synchrotron Radiation in Biology, ed. H.Stuhrmann, Academic Press, Chapter 1

/24/ E.Spiller and R.Feder, X-Ray Lithography, in: X-Ray Optics, ed. H.-J.Queisser, Topics in Appl. Physics Vol. 22, Springer Berlin (1977)

/25/ R.Feder, D.Sayre, E.Spiller, J.Topalian and J.Kirz, J.Appl. Phys. 47, 1192 (1976)

/26/ E.Spiller, R.Feder, J.Topalian, D.Eastman, W.Gudat and D.Sayre, Science 191, 1172 (1976)

/27/ B.Fay, J.Trotel, Y.Pétroff, R.Pinchaux and P.Thiry, Appl. Phys.Lett. 29, 370 (1976)

/28/ F.Polack, S.Lowenthal, Y.Pétroff, Y.Farge, Nucl. Instrum. and Meth. 152, 289 (1978)

/29/ J.Wm.McGowan, B.Borwein, J.A.Medeiros, E.Spiller, R.Feder, J.Topalian and W.Gudat, J.Cell.Biol. 80, 732 (1979)

/30/ P.Pianetta, R.Burg, J.Kirz, H.Rarback, J.Wm.McGowan and M.Malachowsky, Stanford Synchrotron Radiation Laboratory SSRL Report (1979)

/31/ B.J.Panessa-Warren and J.B.Warren, to be published

/32/ for most recent references see also: Conference on Ultrasoft X-Ray Microscopy: Its Application to Biological and Physical Sciences, New York (June 1979), The New York Academy of Science, to be published.

/33/ L.Manuelidis, J.Sedat, R.Feder, IBM Research Report RC 7758 (1979) and to be published

/34/ H.J.Hagemann, W.Gudat, C.Kunz, J.Opt.Soc.Am. 65, 742 (1975) and DESY Report SR 74 7 (1974)

/35/ J.H.Hubbel, Survey of Photon-Attenuation-Coefficient Measurements 10 eV to 100 GeV, Atomic Data 3, 241 (1971); B.L.Henke, E.S.Ebisu, Low Energy X-Ray and Electron Absorption within Solids, AFORS Report 72-2174, Univ. Hawaii (1973); B.L.Bracewell, W.J.Veigele, in: Developments in Applied Spectroscopy, Vol. 9, ed. E.L.Grove and A.J. Perkins, Plenum, New York (1971), p.375

/36/ P.Lamarque, C.R.Acad.Sci. Paris 202, 684 (1936)

/37/ H.Wolter, Ann.der Physik 10, 94 (1952)

/38/ B.L.Henke, in: Advances in X-Ray Analysis, ed. W.M.Müller, Vol. 2, p.117, Plenum Press (1960)

/39/ A.Halpern, in: Uses of Synchrotron Radiation in Biology, ed. H.Stuhrmann, Academic Press, London (1980)

/40/ D.Sayre, J.Kirz, R.Feder, D.M.Kim and E.Spiller, Ann.N.Y. Acad.Sci. 306, 286 (1978)

/41/ W.Gudat and C.Kunz: Instrumentation for Spectroscopy and other Applications,in: Topics in Current Physics, Vol. 10, p.55, ed. C.Kunz, Springer Berlin-Heidelberg (1979)

/42/ Due to the small thickness of the resist layer being used for CM, and due to magnitude of the linear absorption coefficient α of PMMA (see Fig.4), only a small fraction ($\lesssim$ 1%) of the incident flux is absorbed.

/43/ W.A.Ladd, W.M.Hess and M.W.Ladd, Science 123, 370 (1956)

/44/ H.H.Pattee, in: X-Ray Microscopy and X-Ray Microanalysis, eds. A.Engström, V.Gosslett, H.Pattee, p. 61, Elsevier Publishing, Amsterdam (1960)
S.A.Asunmaa, ibid. p. 66

/45/ S.K.Asunmaa, in: X-Ray Optics and X-Ray Microanalysis, eds. H.H.Pattee, V.E.Cosslett and E.Engström, p. 33, Academic Press (1963)

/46/ A) B.Ranby and J.F.Rabak, Photodegradation, Photooxidation and Photostabilization of Polymers, Wiley and Sons, New York (1975)

/46/ B) A.Charlesby, in: Radiation Damage Processes in Materials, ed. C.H.S.Dupuy, p. 231, Noordhoff. Leyden (1975)

/47/ M.Hatzakis, J.Electrochem.Soc. 116, 1033 (1969)

/48/ E.Spiller, R.Feder, J.Topalian, W.Gudat and D.E.Eastman, IBM Research Report, RC 5797 (1976)

/49/ L.Möller, Diploma-Thesis, Universität Hamburg (1979) and W.Gudat, L.Möller, B.Niemann, G.Schmahl, to be published

/50/ M.Hatzakis, Appl.Phys.Lett. 18, 7 (1971)

/51/ R.Feder, E.Spiller and J.Topalian, J.Vac.Sci.Technol. 12, 1332 (1975)

/52/ e.g. C.J.Powell, Surf.Science 44, 29 (1974)

/53/ e.g. A.Sommerfeld, Optik, Akademische Verlagsgesellschaft, Leipzig (1974)

/54/ O.C.Wells, A.N.Broers and C.Bremer, Appl.Phys.Lett. 23, 353 (1973)

/55/ K.Adachi, K.Hojou, M.Katoh and K.Kanaya, Ultramicroscopy 2, 17 (1976)

/56/ B.J.Panessa-Warren and J.B.Warren, to be published in Ref.32

/57/ J.A.Zadunaisky, to be published in Ref. 32

/58/ F.Polack, S.Lowenthal, Y.Pétroff, Y.Farge, Appl.Phys. Lett. 31, 785 (1977)

/59/ J.Sedat, R.Feder, E.Spiller and L.Manuelidis, to be published in Ref. 32

/60/ G.Dupouy, F.Perrier and L.Durrieu, C.R.Acad.Sci.251, 2856 (1960/

/61/ see e.g. D.F.Parsons, Science 186, 407 (1974)

/62/ P.Pianetta, Report of Working Group on X-ray Lithography, SSRL Report No. 78/04, p.IV 1 (1978)

/63/ W.Gudat, Research Proposal DESY 1976

/64/ P.J.Malozzi, H.M.Epstein, R.G.Jung, D.C.Applebaum, B.P.Fairand, W.J.Gallagher, R.L.Uecker and M.C.Muckersheide, J.Appl.Phys. 45, 1891 (1974)

/65/ R.A.McCorkle and H.J.Vollmer, Rev.Sci.Instrum. 48, 1055 (1977)

/66/ J.Gur, J.Opt.Soc.Am. 69, 1415 (1979)

Table 1. Properties of several X-ray resists. Unless noted, the required incident dose F is for λ =0.83 nm. By multiplying F with the linear absorption coefficient α the absorbed dose W is obtained. (after E.Spiller and R.Feder /24/)

RESIST	CHARACTERIZATION	REQUIRED INCIDENT DOSE F (J/cm^2)	REQUIRED ABSORBED DOSE W (J/cm^3)	RESOLUTION Δ (cm)	N ABSORBED PHOTONS/Δ^3
POLYMETHYL METHACRYLATE	$\gamma=2$	0.33	330	35 Å(λ=0.83nm	500
(PMMA), POSITIVE	$\gamma=3-7$	0.5	500	5 Å(λ=4.48nm	1.4
	$\gamma=3$	3.5(λ=0.437nm)	500		
	$d_{NORM}=0.5$	0.07	70		
	$d_{NORM}=0.9$	0.2	200		
COP(MMA-MAA)					
MODIFIED PMMA TO ALLOW DOPING, POSITIVE	$\gamma=1$	0.05	50		
	$d_{NORM}=0.5$	0.01	10		
	$d_{NORM}=0.9$	0.05	50	50	260
TIP(MMA-MAA) POSITIVE	TANβ=5	0.024	80	100	340
POLYBUTADIENE	$d_{NORM}=0.5$	0.04	20		
PB, NEGATIVE	$\gamma_{NORM}=1$				
POLY(DICHLORO PROPYL ACRYLATE)	$d_{NORM}=0.5$				
DCPA NEGATIVE	$\gamma_{NORM}=0.85$	0.0078 (FOR λ=0.437 nm)	10	0.5 µm	5000
EPOXIDIZED POLYBUTADIENE	$d_{NORM}=0.5$	0.0015	1	1 µm	4000
NEGATIVE	$\gamma_{NORM}=0.56$				

Figure Captions

Fig.1 Principle of microradiography: I The incident X-ray flux is modified by the optical density of the specimen and absorbed in the X-ray resist. II After removal of the specimen a resist repica of the specimens optical density is obtained in a wet development procedure. This is examined in a scanning electron microscope after metallization.

Fig.2 Replica of diatoms obtained with synchrotron radiation with an effective wavelength range 25 nm to 44 nm. Exposure time 10 min in a distance of 40 m from the source point. Effective exposure about 1200 J/cm^3. (from Spiller et al /26/)

Fig.3 Schematic diagram of the experimental set-up for contact-microradiography at DESY. At the sample chamber a horizontal angle from the source corresponding to 1 mrad can be used for exposures. Several specimen, premounted on resist-wafer-substrates, and fixed to sample wheels, can be exposed during one pump-down cycle.

Fig.4 Linear absorption coefficient of various materials in the soft X-ray range. PMMA (polymethylmethacrylate) is a positive X-ray resist. Note, that the absorption coefficient of biological material is considerably smaller in the range 2.3 nm to 4.4 nm than that of water allowing for an investigation of wet specimen.

Fig.5 a) For a model specimen consisting of a protein feature in a water background, as shown in the in-set, the minimum exposure is shown which produces a signal to noise ratio of 5 in a transmission microscopy mode. Wavelength regions corresponding to minimum radiation damage are indicated by dashed lines.

b) The flux levels shown in a) are converted to the specimen dose allowing for an easier comparison e.g. with electron beam damaging (after Sayre et al /3/).

Fig.6 Dissolution rate versus exposure for PMMA resist developed in methyl isobutylketone (MIBK) and isopropyl alcohole (IPA). The contrast of the resist, i.e. the slope of curve segments, is seen to depend on exposure and development procedure (from Spiller and Feder /24/).

Fig.7 Resist pattern obtained in thick resist with X-rays of o.45 nm wavelength. The linewidth is 1 um, i.e. only a small fraction of the resist thickness. In X-ray lithography these high aspect-ratios are important (by courtesy of E.Spiller).

Fig.8 Latex spheres of o.5 μm diameter are imaged with monochromatized (λ=(4.6±0.1)nm) and focussed (by means of zone plates) synchrotron radiation. The upper part shows replica in PMMA resist which are well exposed and appropriately developed. The lower part shows distorted replicas due heavy overexposure closer to the center of the focal spot. The fine substructure of size 70 nm is due to the collodian support of the latex spheres (from Möller et al /49/).

Fig.9 The dissolution rate of PMMA versus the convenient exposure time scale displays different slopes in different spectral ranges, indicating a photon energy dependence of the contrast of PMMA.
A: full spectrum B: spectrum after 4°grazing incidence reflection C: as B plus additional 0.3 μm PMMA filter D: as B plus additional filter 0.3 μm PMMA and 0.05μm Ag /49/.

Fig.10 Fresnel type diffraction is evident in the PMMA replica of the edge of a Cu grid (part a) and in the replica of a 0.5 μm latex sphere. A focussed beam of soft X-rays (λ=4.6±1nm) was used for exposure. The grid and the specimen were not in contact with the resist /49/.

Fig.11 The normalized intensity distribution in case of Fresnel diffraction is shown. An enhancement of diffraction extrema is due to the contrast factor γ of the resist and is indicated by the dashed line.

Fig.12 With broad band synchrotron radiation (~2.0 to 4.4 nm) a replica has been obtained from a thin (~70 nm) plastic embedded section of frog retinal pigment epithelium. Part a) shows blurred structures of elliptical type melanin granules, obtained with a commercial SEM. In contrast, in part b) a high resolution SEM micrograph shows details of a melanin granule with dimensions of about 10 nm. This is close to the expected diffraction limit (from Feder et al /13/).

Fig.13 Heart of chick embryo cells are replicated with synchrotron radiation and with carbon K_α radiation. Nucleus (N), nucleolus (NO), microspikes (MS) and microtubules (MT) are identified. C denotes cell fragments due to incomplete removal of the specimen The prominence of the nucleus in the lower replica is ascribed to build up of phosphorus which gives higher contrast with 4.4 nm wavelength than with wide band synchrotron radiation (from McGowan et al /29/).

Fig.14 Carbon K_α soft X-ray micrograph in PMMA resist shows edge of a nucleus. Stacking of components in two large vertical 220-270 nm features is seen (large arrowheads). Substructure of ~60 nm is also identified (small arrows). (from Manuelidis et al /33/).

Fig.1

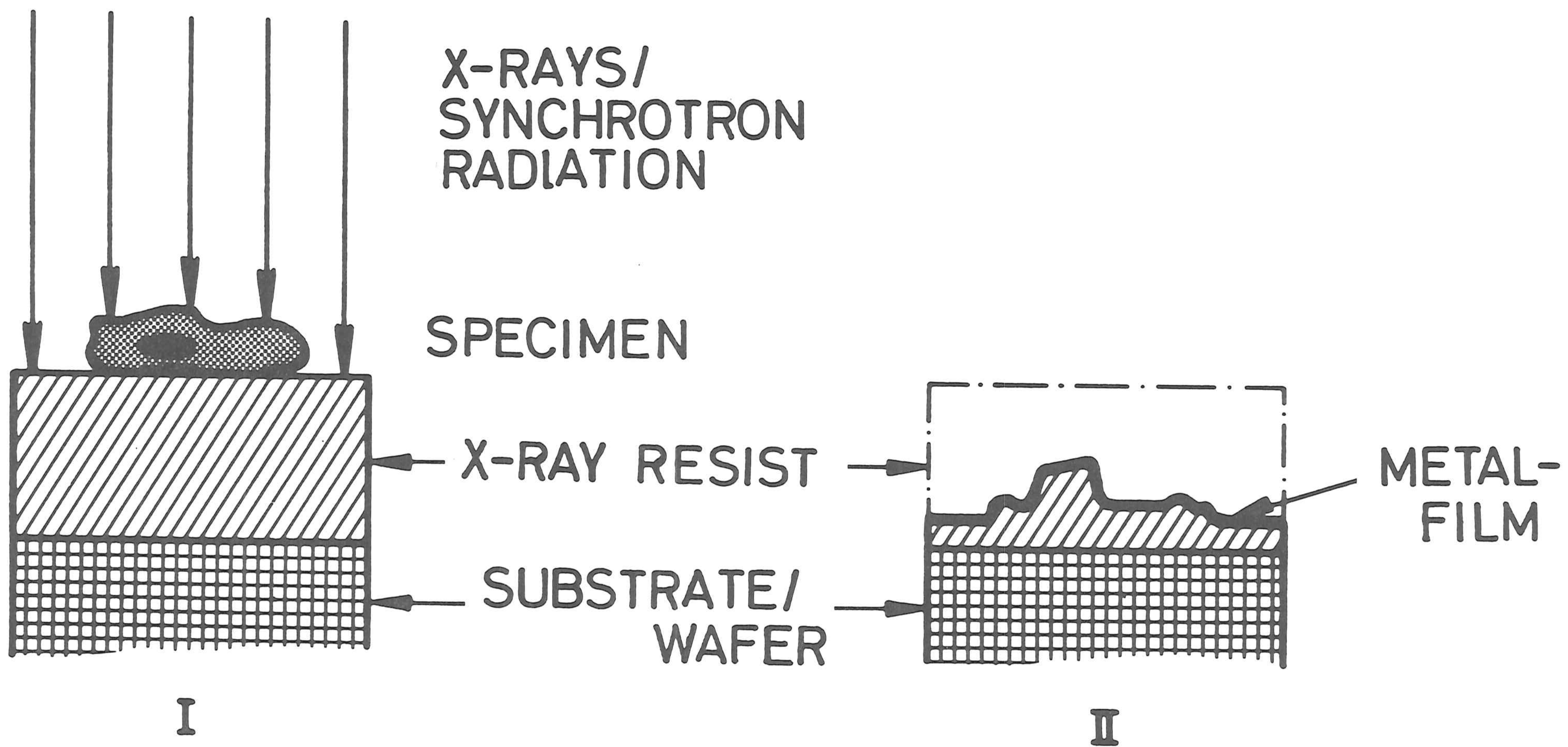

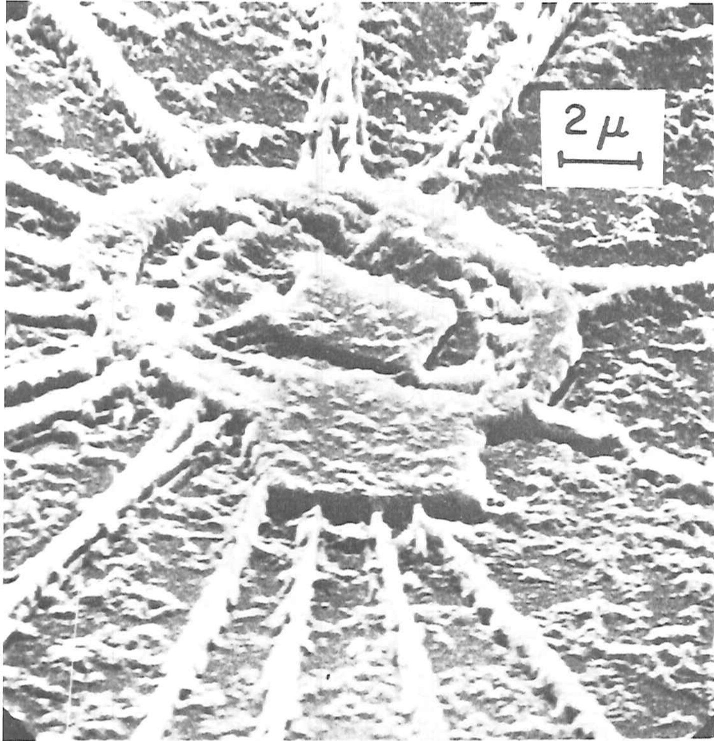

a

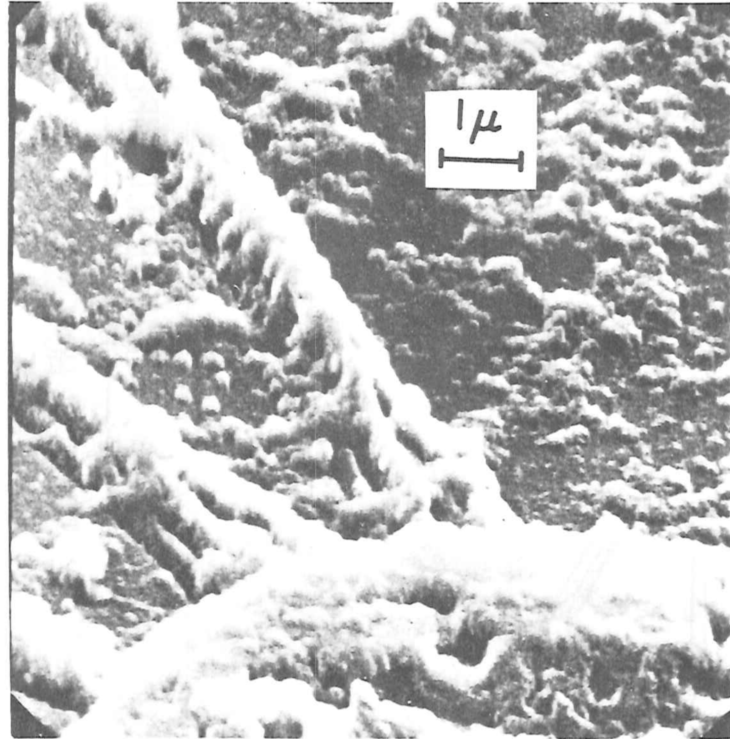

b

Fig.2

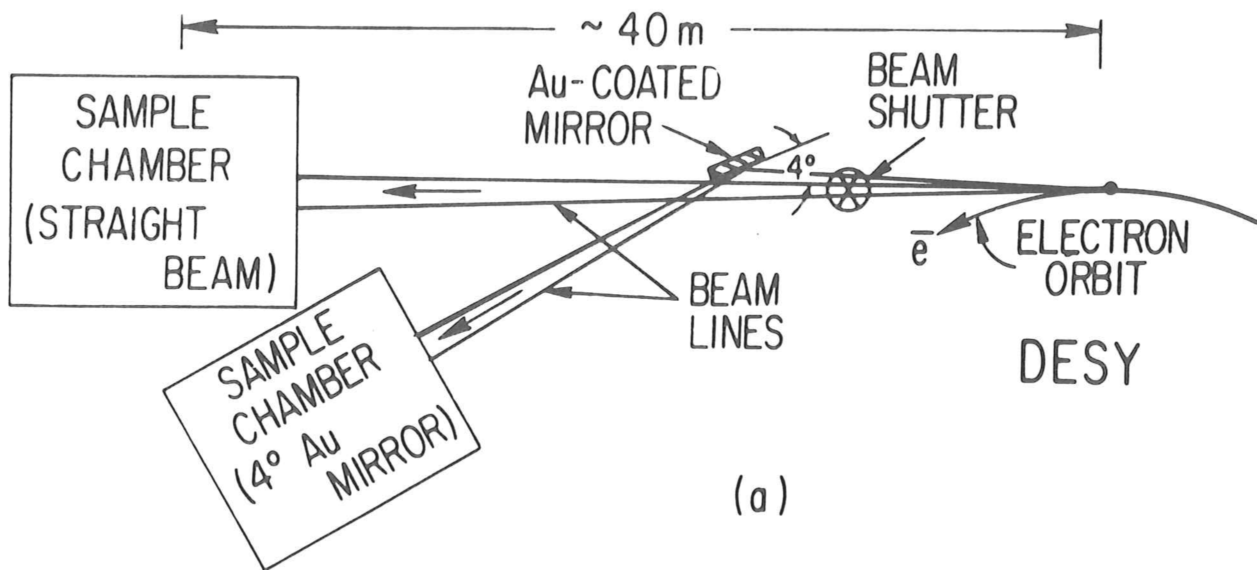

(a)

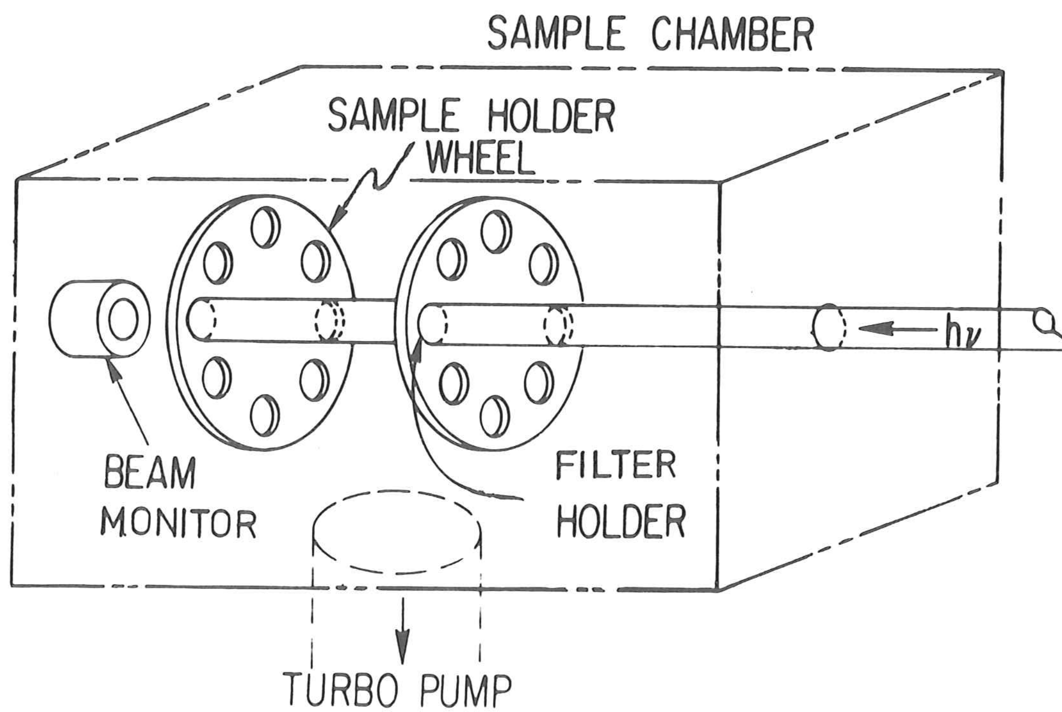

(b)

Fig.3

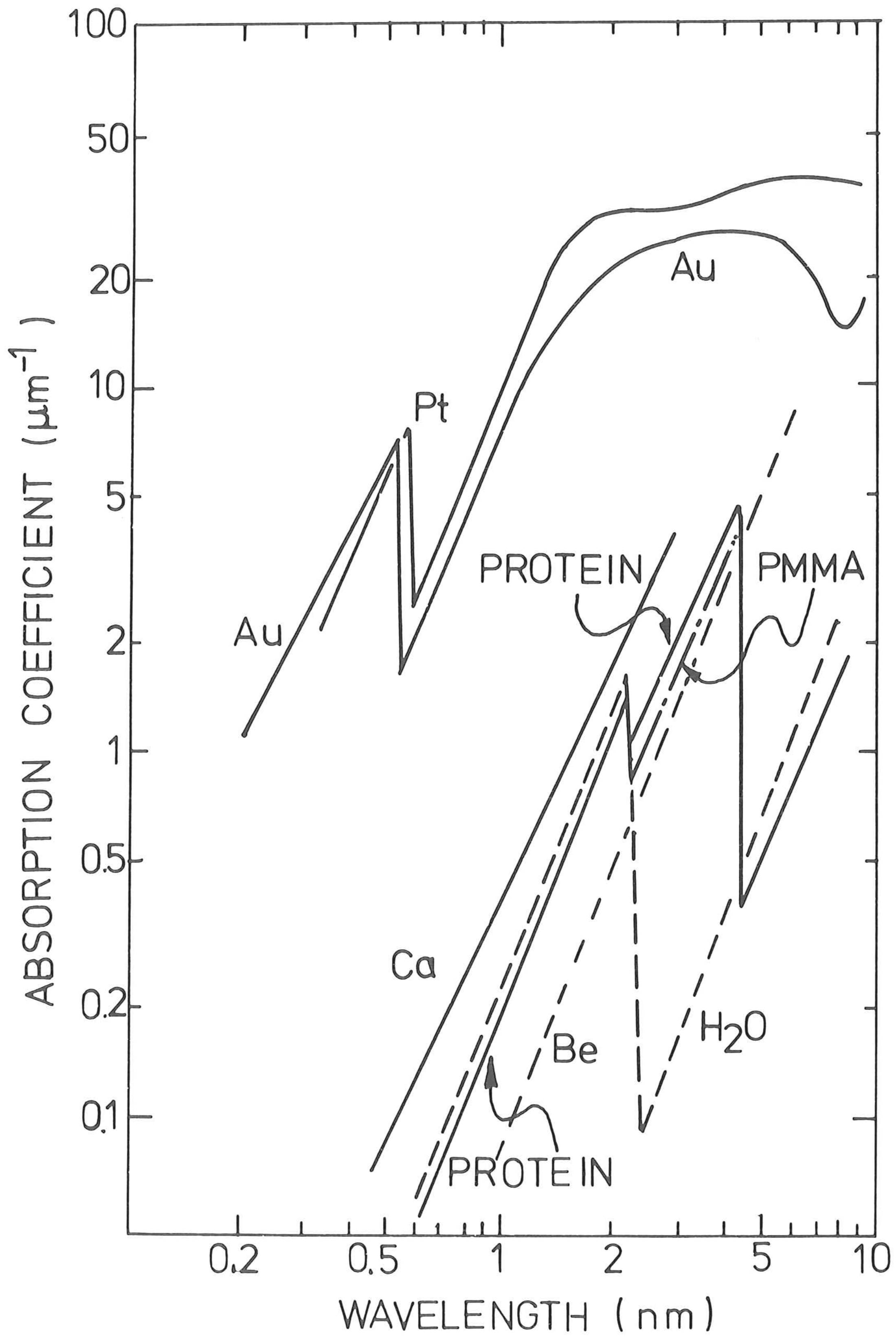

Fig.4

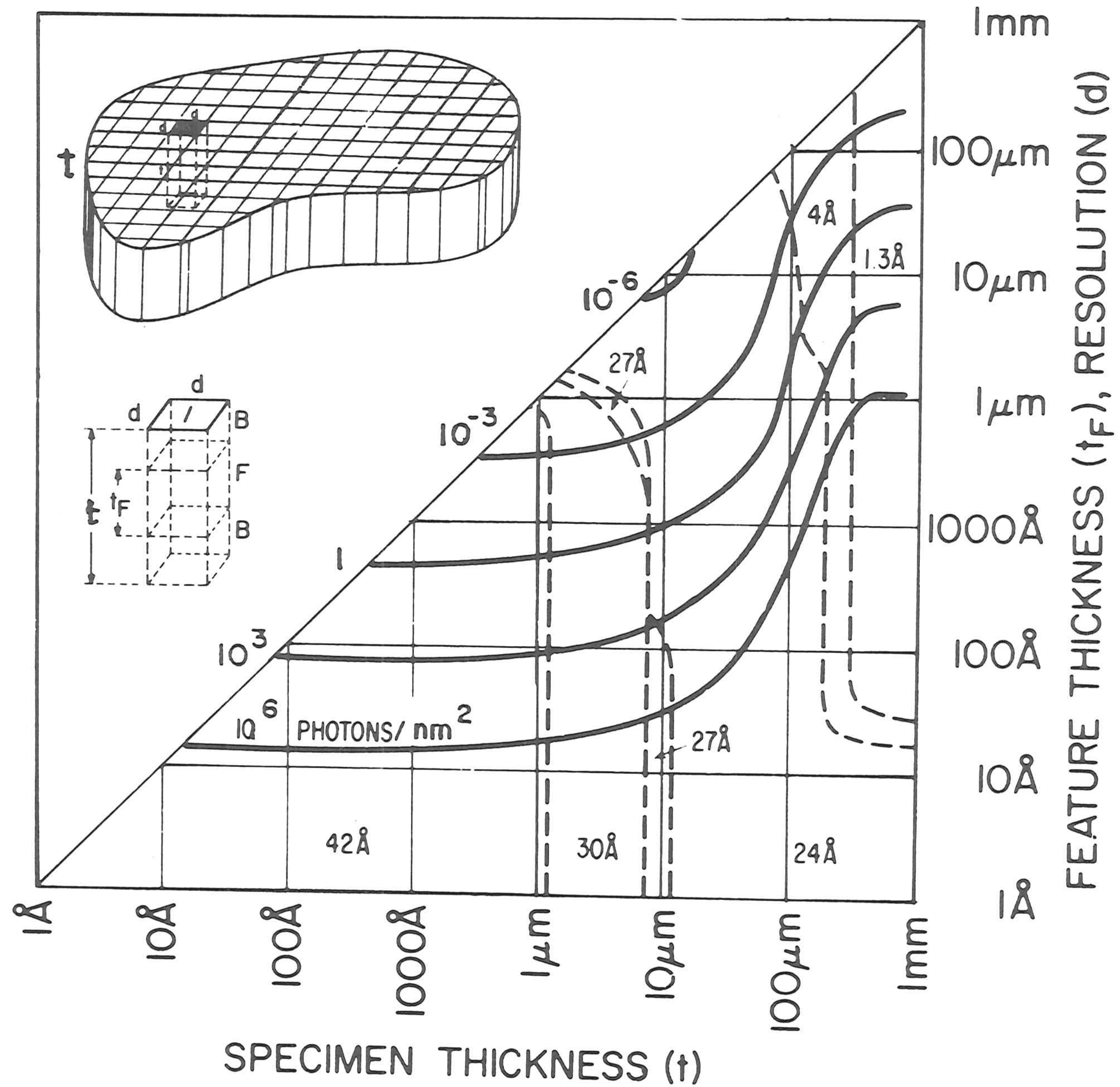

Fig. 5a

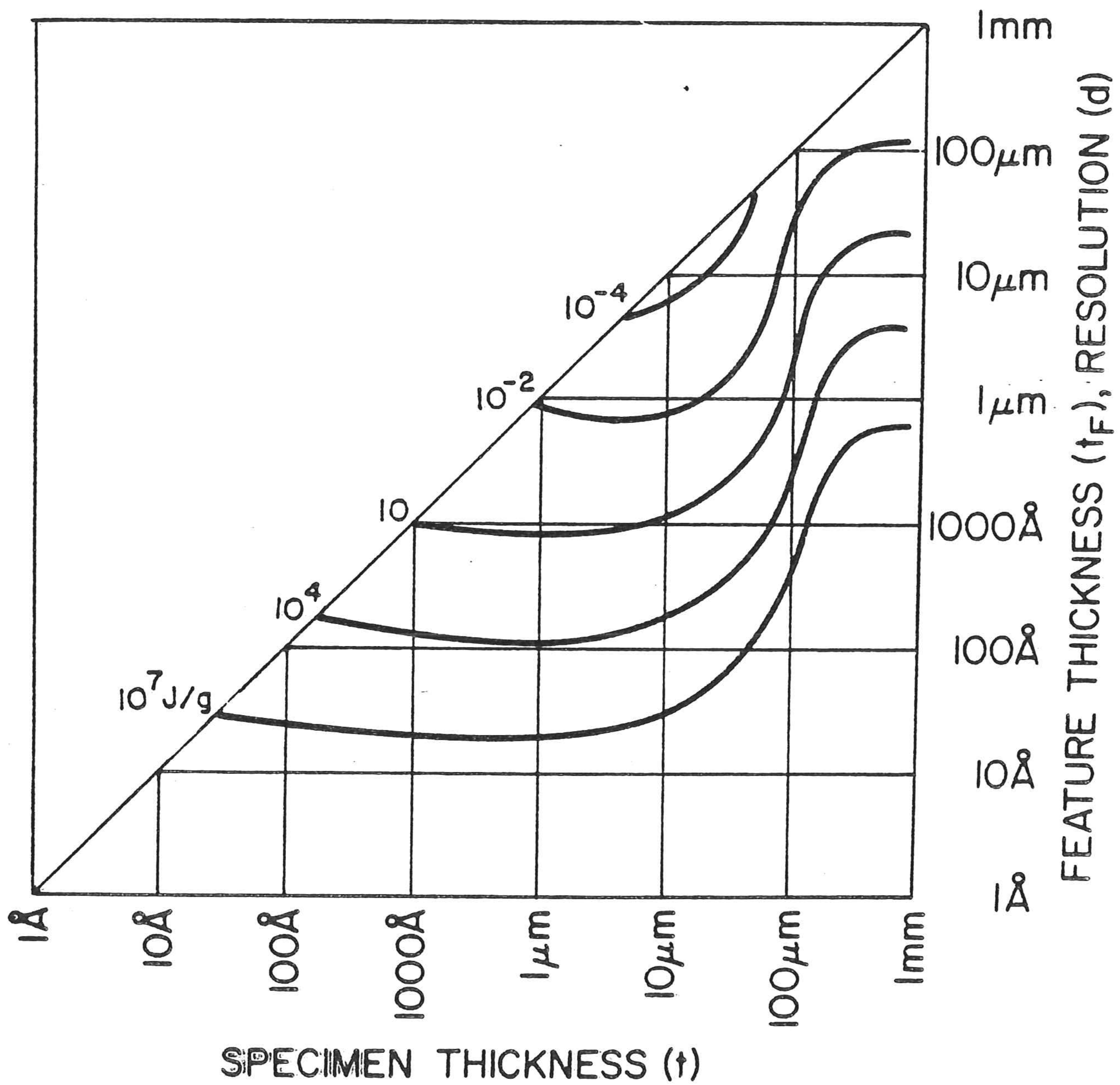

Fig. 5b

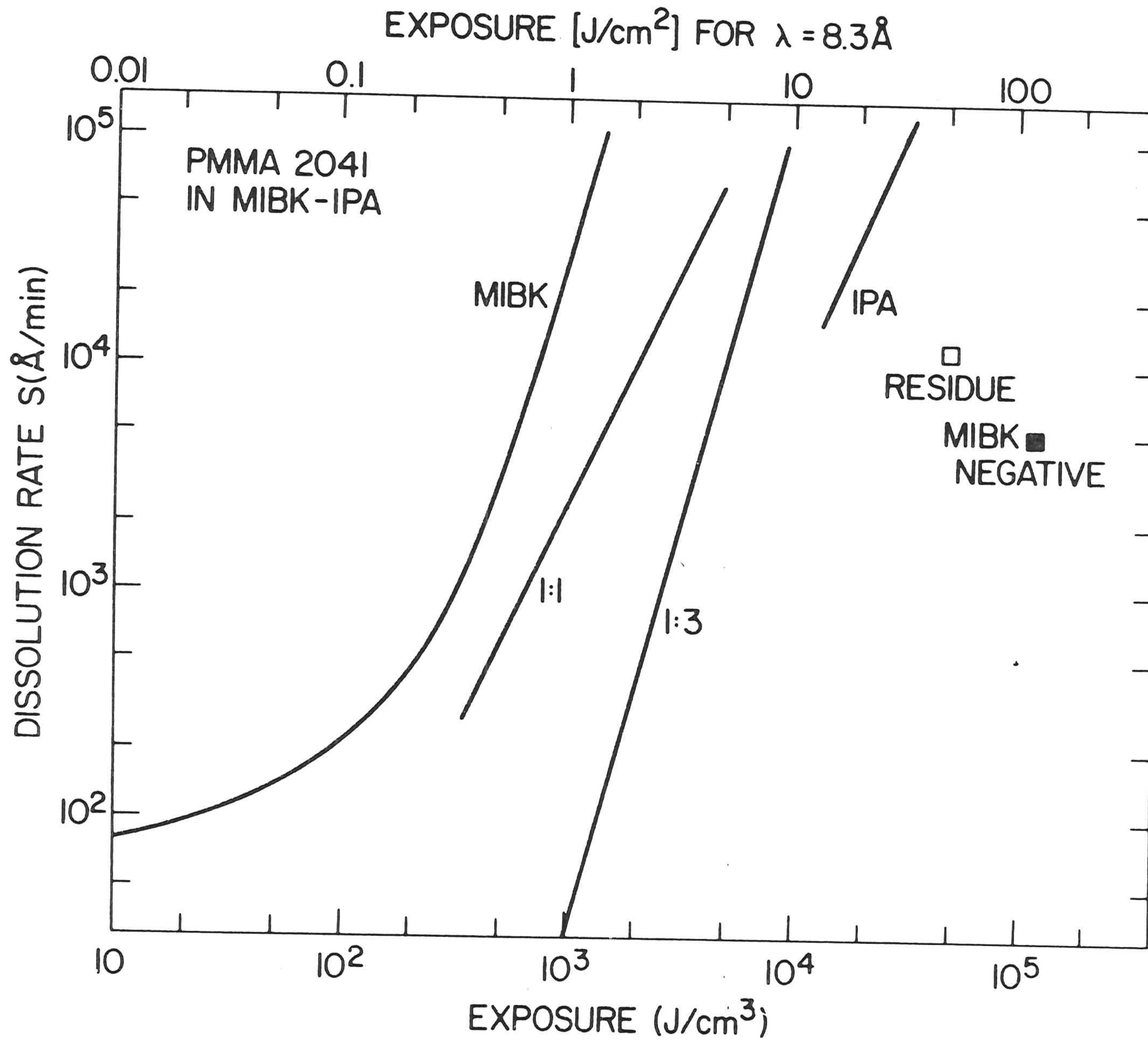

Fig. 6

Fig.7

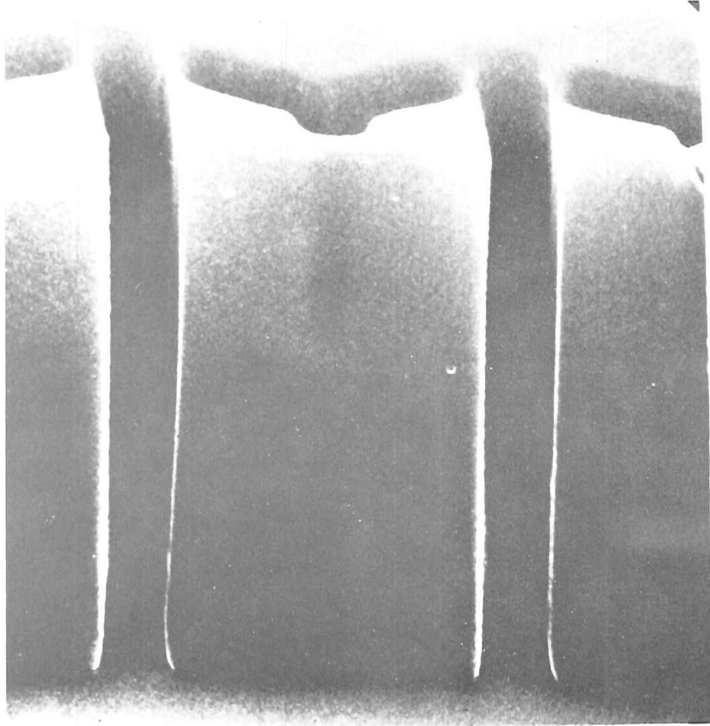

(a)

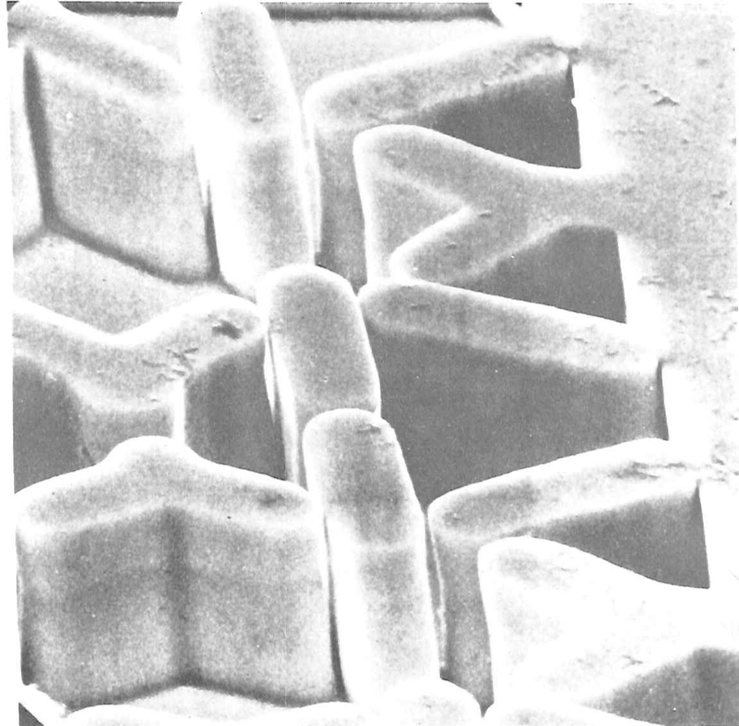

(b)

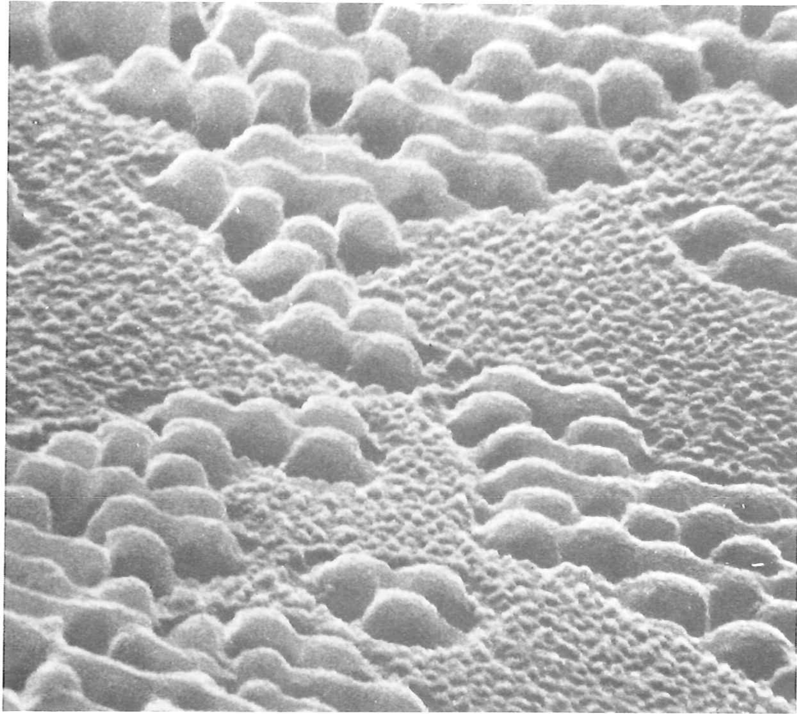

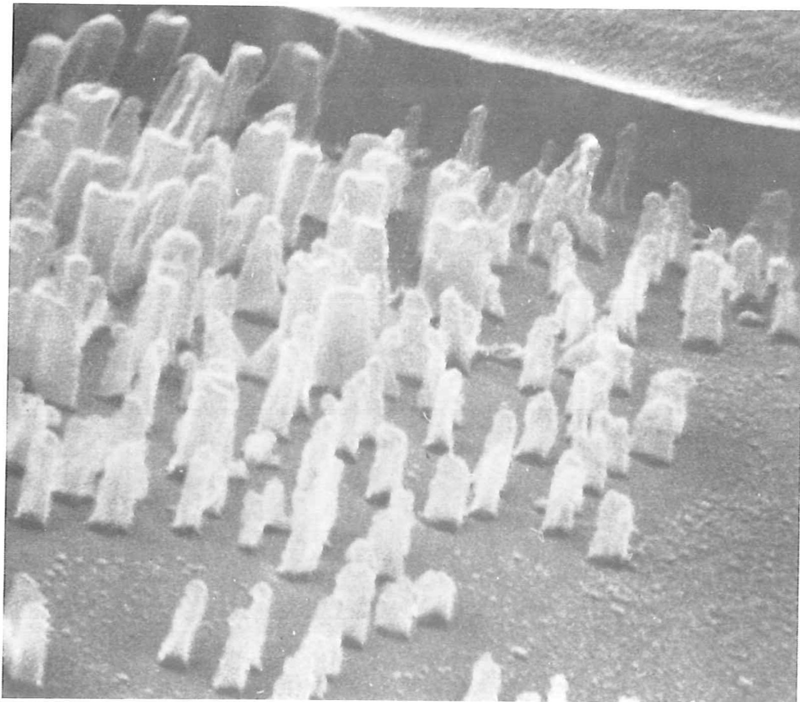

Fig.8

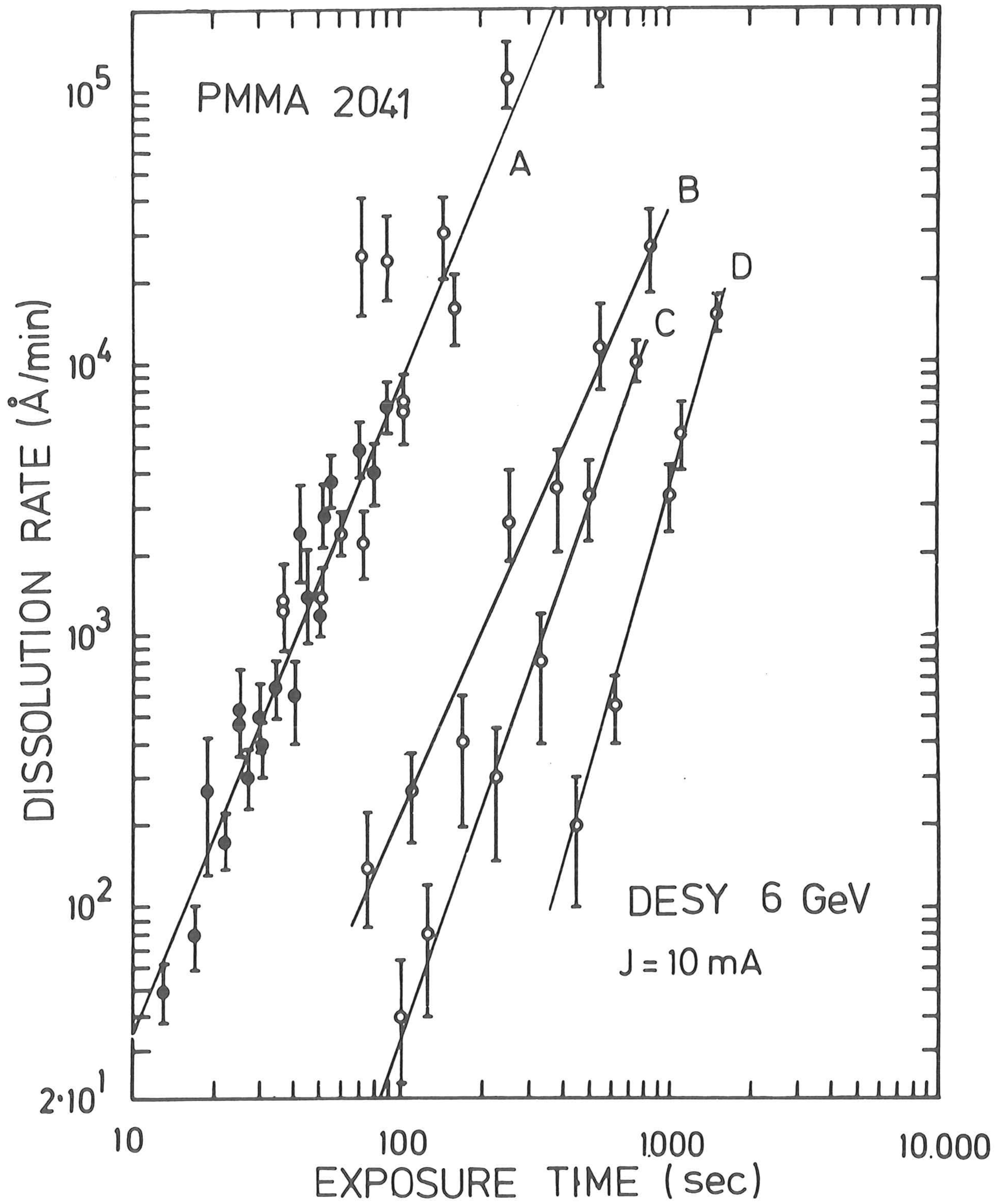

Fig.9

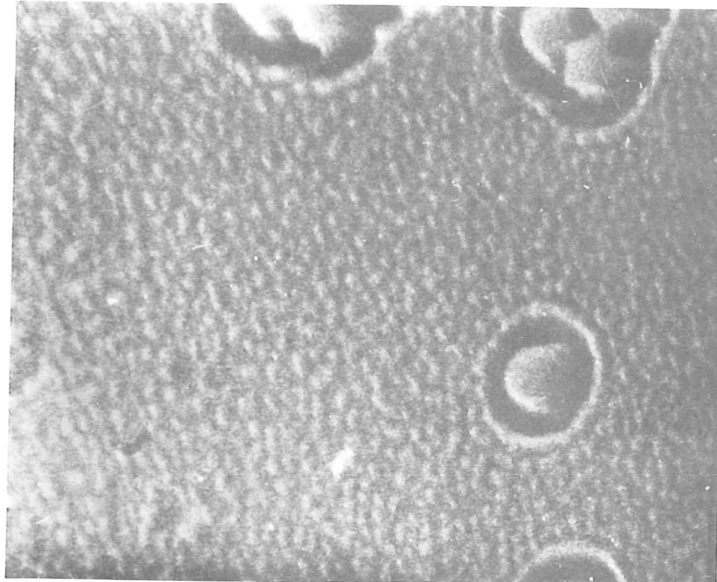

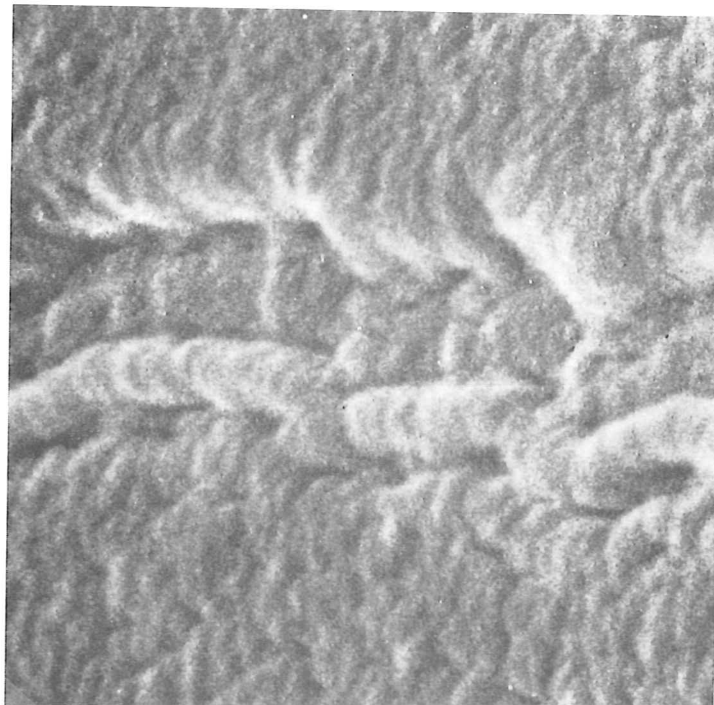

Fig.10

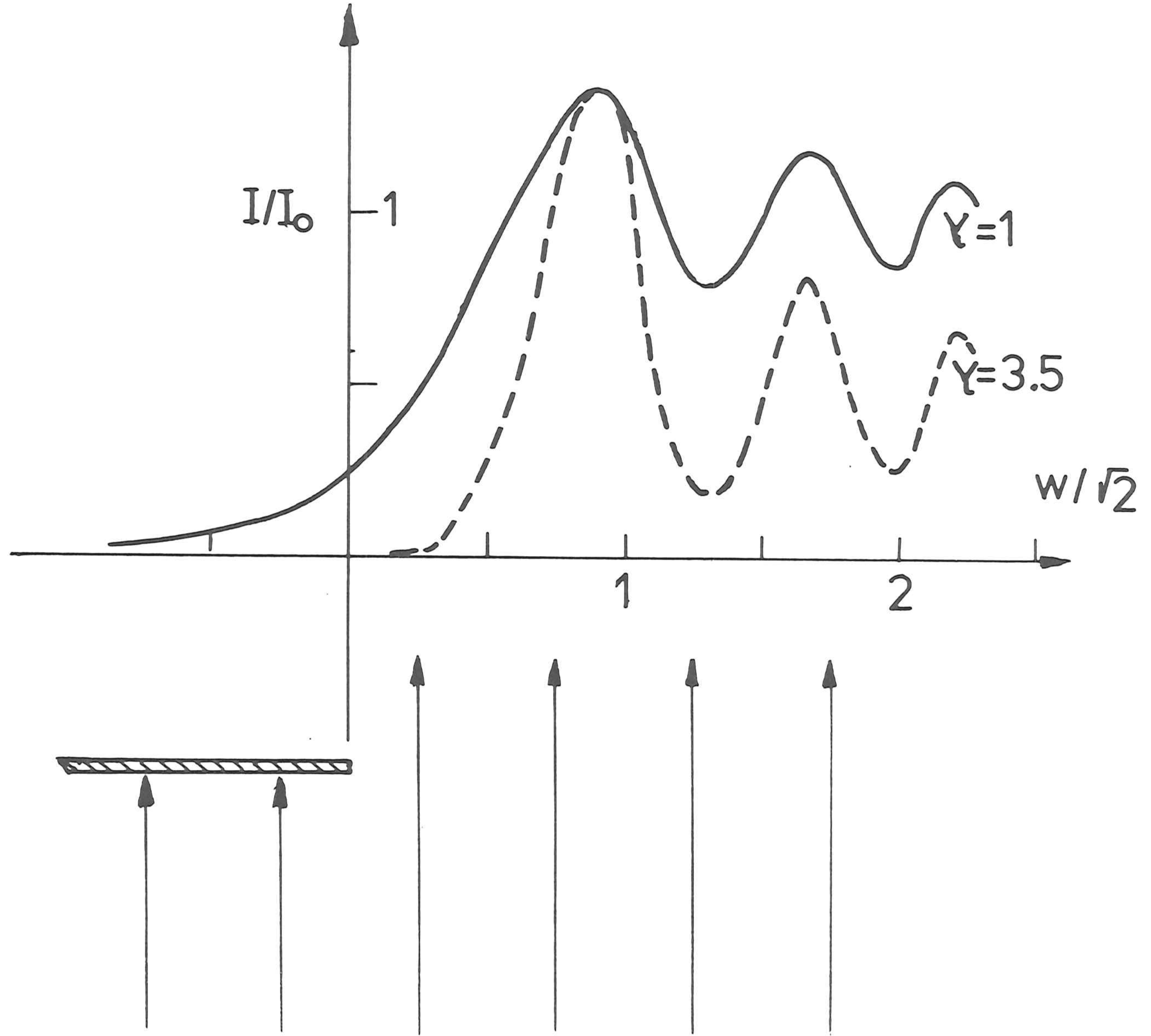

Fig. 11

Fig. 12

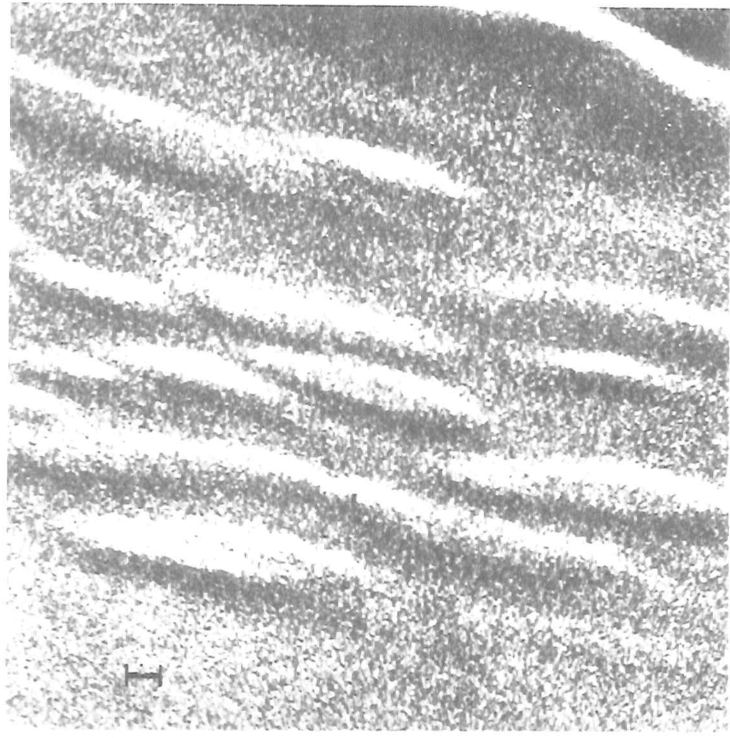

a

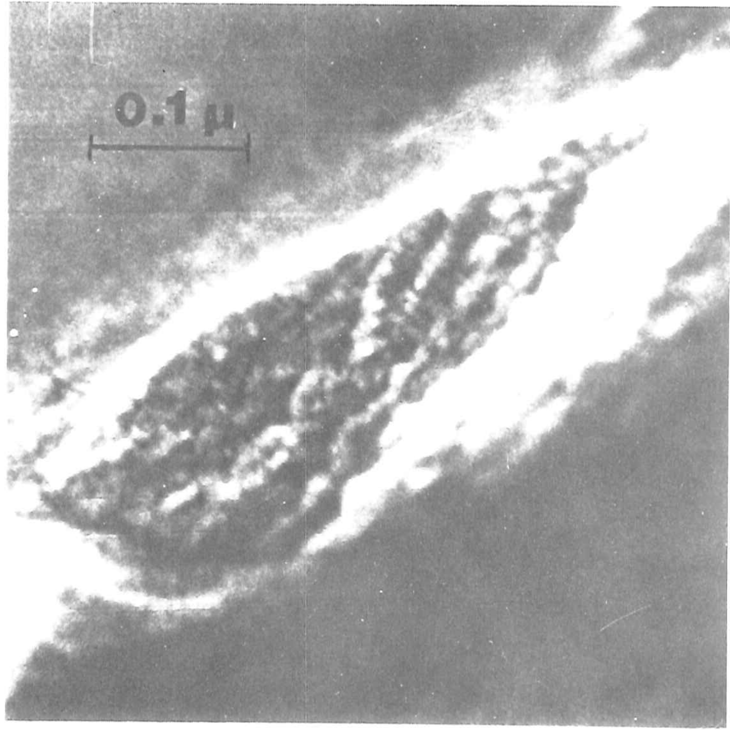

b

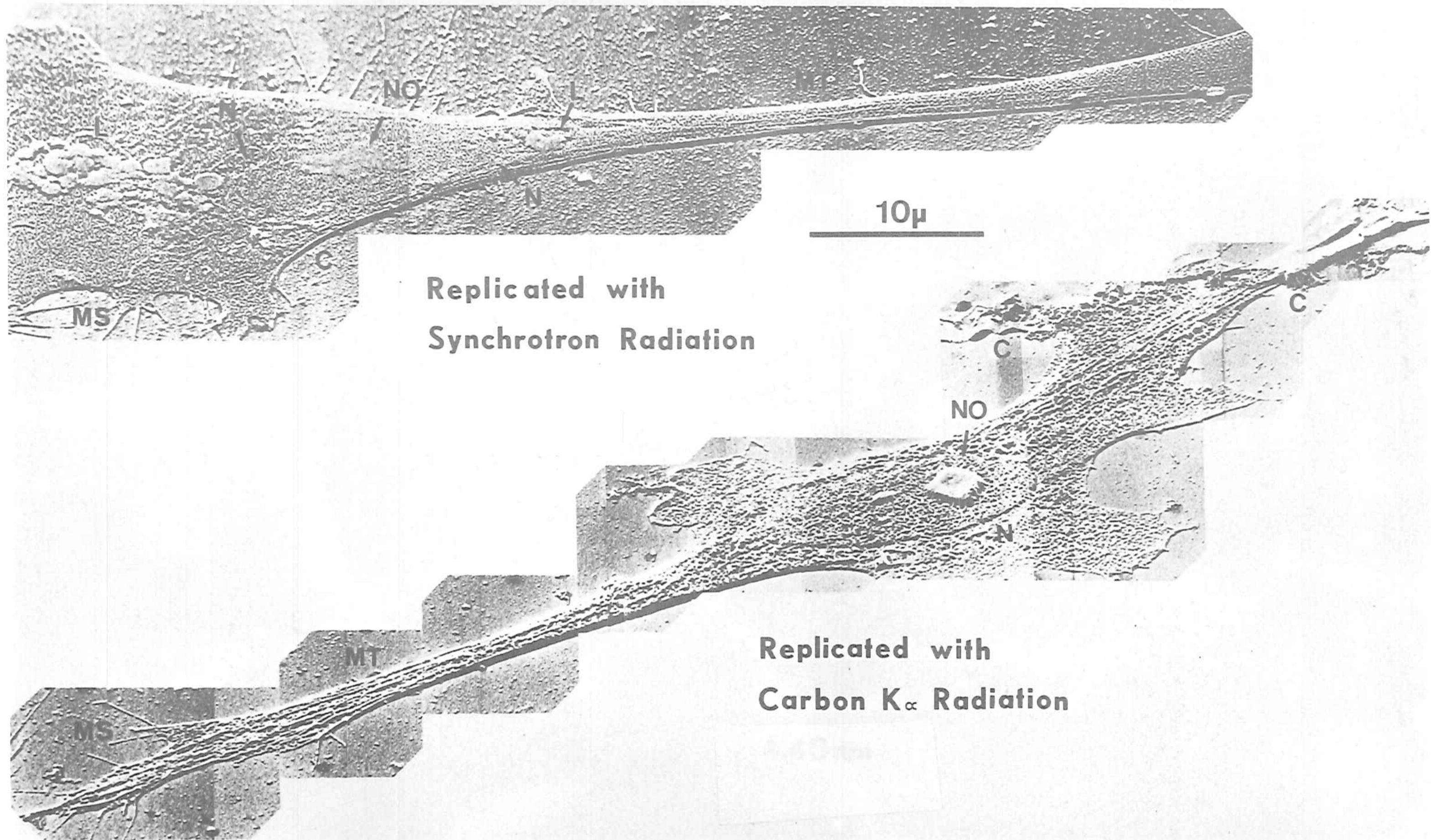

Fig. 13

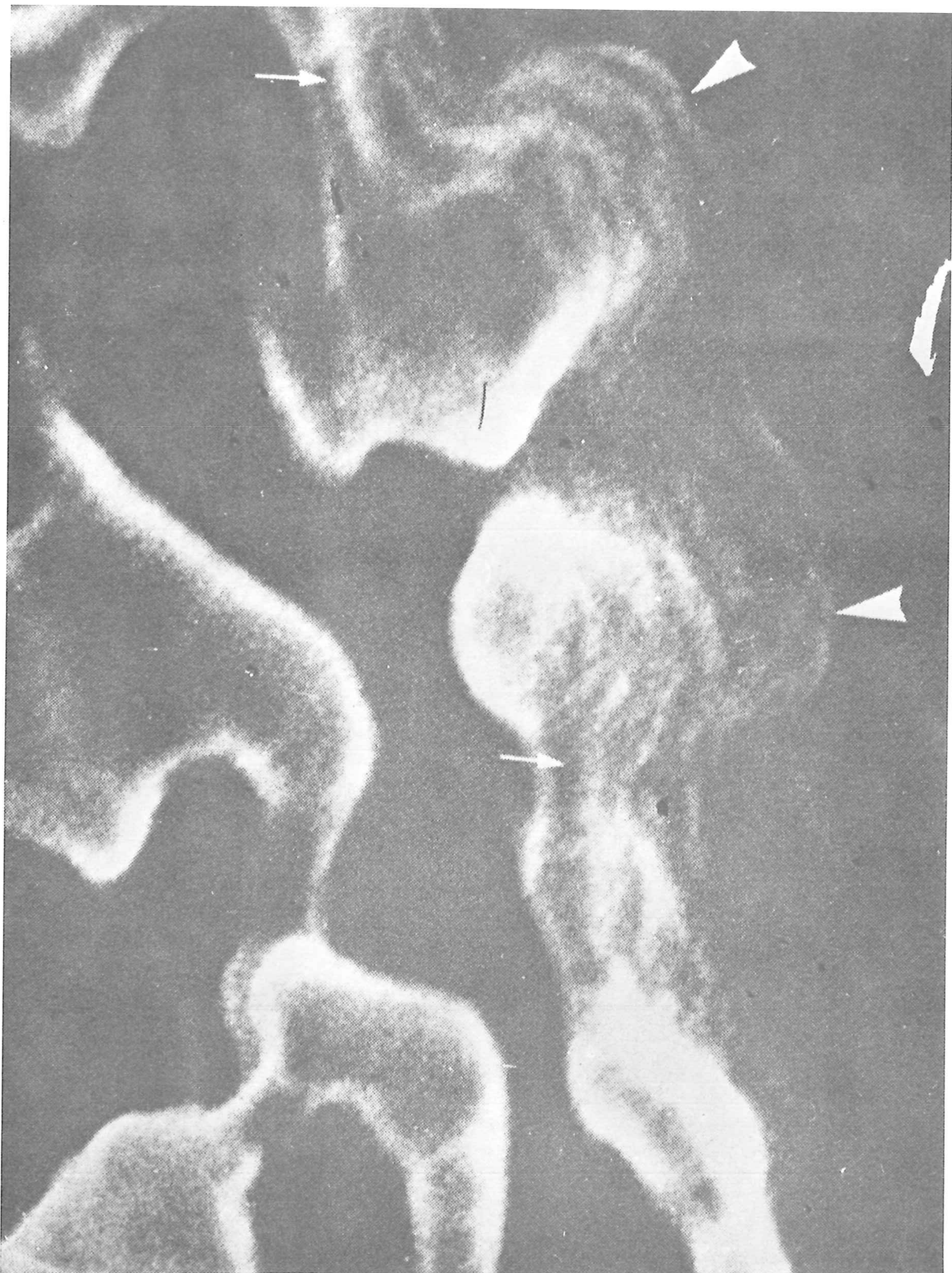

Fig. 14